



HAL
open science

Twist control of aerodynamic profiles by a reactive method (experimental results)

Jean-Baptiste Runge, Daniel Osmont, Roger Ohayon

► **To cite this version:**

Jean-Baptiste Runge, Daniel Osmont, Roger Ohayon. Twist control of aerodynamic profiles by a reactive method (experimental results). *Journal of Intelligent Material Systems and Structures*, 2012, 24 (8), pp.908-923. 10.1177/1045389x12437884 . hal-03177495

HAL Id: hal-03177495

<https://hal.science/hal-03177495v1>

Submitted on 29 Aug 2023

HAL is a multi-disciplinary open access archive for the deposit and dissemination of scientific research documents, whether they are published or not. The documents may come from teaching and research institutions in France or abroad, or from public or private research centers.

L'archive ouverte pluridisciplinaire **HAL**, est destinée au dépôt et à la diffusion de documents scientifiques de niveau recherche, publiés ou non, émanant des établissements d'enseignement et de recherche français ou étrangers, des laboratoires publics ou privés.

Twist control of aerodynamic profiles by a reactive method (experimental results)

Jean-Baptiste Runge¹, Daniel Osmont¹ and Roger Ohayon²

Abstract

Active twist control of airfoils using embedded actuators has been widely studied during the last decade. To control the twist, an additional torsional moment is applied using these actuators. This active method is efficient but encounters limitations due to the amount of energy necessary to activate the system. An alternative method to this energy costly active control is proposed. Rather than applying an additional torsional moment to control the twist of the structure, the shear center of the profile is shifted using an internal mechanical system. More precisely, the activation of a clutch-like device, able to link or unlink thin internal walls, allows the redistribution of the bending and torsional shear stresses. This process leads to a possible twist control of the airfoil, significantly less energy consuming than an active one. Unlike the active twist control method, this method needs an external force to be effective, so it is called a “reactive” control method. Experimental investigations have been performed to verify the efficiency of this method. The results show that it is possible to obtain significant twist angle modifications. Moreover, the measurement of internal longitudinal displacements, correlated with the twist angle, enables the twist control of the structure.

Keywords

Twist, torsion, shear center, reactive method, aerodynamic profile

Introduction

When an airfoil is immersed in an air flow, it is mainly subjected to aerodynamic forces called lift and drag forces. The local density of these forces highly depends on the angle of attack of the airfoil in any cross section. In a first approximation, an airfoil may be considered as a rigid structure with an initial angle of attack. To optimize its performances by, for example, maximizing its lift or minimizing its drag, it is necessary to consider its deformations due to aerodynamic forces. The predominant deformations in this situation are bending and torsion. These deformations are generally comprised of a static and a dynamic component and modify the aerodynamic forces. More precisely, the static torsional deformation induces a change in the angle of attack that in turn modifies the local densities of the lift and drag forces. Without inserting a system to modify the twist of the airfoil, the aerodynamic performances can then only be optimized for one flight condition, for example, the cruise flight.

A widely used method to have extended optimized performances is to control the torsional deformation (static and dynamic) by inserting actuators in the airfoil. Through those actuators, an additional external

torsional moment can be applied to increase or reduce the twist of the structure. Several solutions are proposed in the literature, the review of Barbarino et al. (2011) detailed past and current developments in terms of morphing aircraft, including twist control methods. We can quote in particular work of Antcliff and McGowan (2000), Bueter et al. (2000), Atulasimha and Chopra (2003), Mistry et al. (2011), Riemenschneider et al. (2004), and Wierach et al. (2005). Proposed systems were based on active control methods and led often to successful prototypes. Although the active control method is very effective, it is also energy consuming. Indeed, all existing kinds of actuator used for active twist control require an energy proportional to the torsional elastic energy stored in the structure. During the past few years, technical progress in the

¹ONERA, DMSC, Chatillon, France

²Conservatoire National des Arts et Metiers (CNAM), LMSSC, Paris, France

Corresponding author:

Jean-Baptiste Runge, ONERA, DMSC, BP72, 29 avenue de la Division Leclerc, Chatillon 92320, France.

Email: jean-baptiste.runge@centraliens-lille.org

field of intelligent materials has been made enabling the integration of compact actuators in the structure of the airfoil to perform morphing wing processes. Despite those advances, the actuator efficiency has a maximum of 50% because of the impedance matching condition (Chopra, 2002). Moreover, without any locking system, maintaining the airfoil in its optimal shape is energy consuming. Finally, to have an effective control system, the input of energy has to be lower than the gain of energy obtained by the activation of the adaptive structure. To get around the energy issue, another idea is to control the twist using flexible wings (Pendleton, 2000). In this case, where a particular twist angle is required, the amount of energy needed to control the angle is lower than the amount of energy needed by the stiffer wings. On the other hand, the structure is even more deformed by the aerodynamic forces, and the active twist control system needs more energy to be activated. These two strategies suggest that an optimized adaptive structure in terms of energy consumption must have two different behaviors: a permanent stiff behavior to avoid deformations and an occasional flexible behavior to allow shape control of the airfoil.

A recent concept is to make use of existing forces as a source of energy. Instead of creating new forces to artificially force the profile to deform itself, already existing forces could be used. Original internal systems have been designed to take advantages of those forces. The rotor blade designed by Gandhi (2009) has a variable span depending on the centrifugal forces. On the other hand, Cooper (2006) proposed to add moving spars in the internal structure to control the twist. This mechanism changes the torsional stiffness and the location of the shear center, modifying indirectly the angle of attack of the profile. The first theoretical analyses show that this method is effective.

The method proposed in this study is close to the latest approach where the twist is controlled by an

internal mechanical system that shifts the shear center. After the concept of the reactive control method being described and justified, experimental proofs of concept are given to show the feasibility of this twist control concept. The purpose is indeed to confirm experimentally the potential of the proposed method. To reach this objective, three demonstrators have been designed consecutively, each time with a greater complexity of the control system. For the first system, the structural modifications are done by hand to simplify the manufacturing of the demonstrator. Its purpose is to determine the order of magnitude of the twist angle changes. The second demonstrator, also activated by hand, focused on the characterization of the activation system. Torsional characteristics like the location of the shear center resulting from the internal modifications have been evaluated. Finally, a third structural demonstrator has been designed to show the possibility of remote activation of the reactive system.

Concept of reactive control

Description of a generic aerodynamic profile

To describe the concept of the reactive control method used in this article, we consider a generic aerodynamic profile. One of the beam tips is clamped on a rigid wall and the other is free (Figure 1(a)), such that, from the structural point of view, it is considered as a cantilever beam. All the cross sections $\Sigma(z)$ are identical, and Figure 1(b) shows that the internal structure is made of a continuous external skin with upper and lower parts joined together by three vertical internal thin walls. The thickness e of this thin-walled structure is assumed to be uniform. The axes x and y are chosen as the principal axes of inertia, and their intersection C_e is the centroid of the cross section.

Pressure forces $p \cdot \mathbf{n}$ are acting on the aerodynamic surface inducing bending and torsion. Their resultant

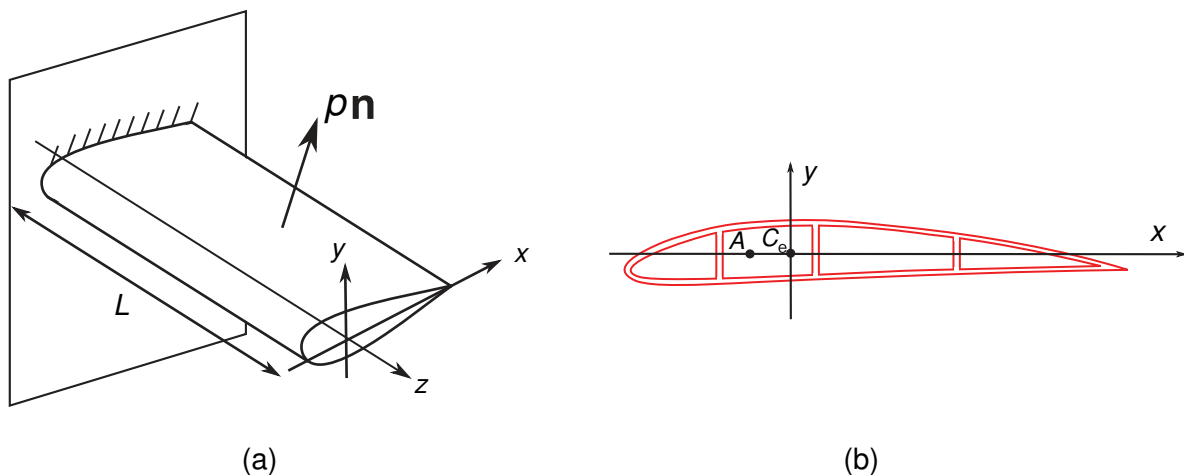


Figure 1. Generic aerodynamic profile. (a) boundaries conditions of a cantilever beam and (b) internal structure.

in each cross section is mainly the lift and drag forces applied at the aerodynamic center A .

Torsional moment

To study torsional mechanisms, we focus on the analysis of the internal equilibrium of stresses acting on each cross section, and more particularly on transverse shear stresses τ .

For each cross section $\Sigma(z)$, we introduce the resultant R_{ext} and the moment M_{ext} of the pressure forces applied to the profile between the sections $\Sigma(z)$ and $\Sigma(L)$. The projection of R_{ext} on the cross-section is the shear force Q , and the components of the moment M_{ext} on the axes $C_e x$, $C_e y$, and $C_e z$ are, respectively, the two bending moments M_x and M_y and the moment M_z .

The distribution of stresses due to the bending of the beam has two components: the normal stress σ_B and the transverse shear stress τ_B . According to the classical Euler–Bernoulli theory, the normal stress depends on the bending moments and on the geometry of the cross section and is written as

$$\sigma_B(x, y) = \frac{M_x}{I_x} y - \frac{M_y}{I_y} x \quad (1)$$

where I_x and I_y are the moment of inertia.

The distribution of bending transverse shear stresses τ_B results from the mechanical equilibrium equation

$$\frac{\partial \tau_{B,x}}{\partial x} + \frac{\partial \tau_{B,y}}{\partial y} + \frac{\partial \sigma_B}{\partial z} = 0 \quad (2)$$

The resultant of stresses τ_B in the cross section is of course equal to the external shear force Q . On the other hand, the moment M_B of stresses τ_B with respect to the z -axis is generally different from the external moment M_z . Therefore, the distribution of stresses $\tau = \tau_B$ is not sufficient to balance both the shear force Q and the external moment M_z . To ensure the equilibrium of the moments along the z -axis, we superpose to the distribution of shear stresses τ_B another distribution τ_T given by the Saint–Venant theory. Its resultant is null, and its moment is the torsional moment $M_T = M_z - M_B$. The complete distribution of shear stresses $\tau = \tau_B + \tau_T$ balances now both the shear force Q and the external moment M_z .

It can be shown that the torsional moment $M_T(z)$ is the moment of external forces with respect to a specific point of the cross section $\Sigma(z)$ called the shear center C_s (equation (3)). The location of this point depends on the distribution of shear stresses and therefore, on the geometry of the cross section. The torsional moment, then, can be written as

$$M_T = M_z + (x_{C_s} - x_{C_e})Q_y - (y_{C_s} - y_{C_e})Q_x \quad (3)$$

In practice, for aerodynamic profiles, only the term depending on the lift force amplitude is considered in

the relation (3). Therefore, the torsional moment is written as $M_T = DQ_y$, where $D = x_{C_s} - x_A$ is its lever arm, that is, the distance between the shear center C_s and the aerodynamic center A .

“Opening” and “closing” walls

It is possible to change the shear center location by modifying the internal geometry of the cross section, for example, moving the walls along the chord direction Cooper (2006). But, this location is difficult to change once the internal geometry of the profile has been chosen. Despite those difficulties, the method proposed here to control the twist will involve a change of its location. Instead of modifying the internal geometry, we propose to modify the distribution of shear stresses τ by changing the topology of the cross sections, for example, the continuity of the internal walls.

In the configuration shown in Figure 2(a), all the walls are continuous. The shear center is at the location C_0 , and the twist due to the torsional moment $M_{T,0} = D_0 Q_y$ is θ_0 . By cutting the rear wall uniformly in the middle plane from one tip of the beam to the other (Figure 2(b)), the topology of the profile is changed showing a discontinuity in the wall. In this case, the shear center C_1 is different from C_0 , and the twist θ_1

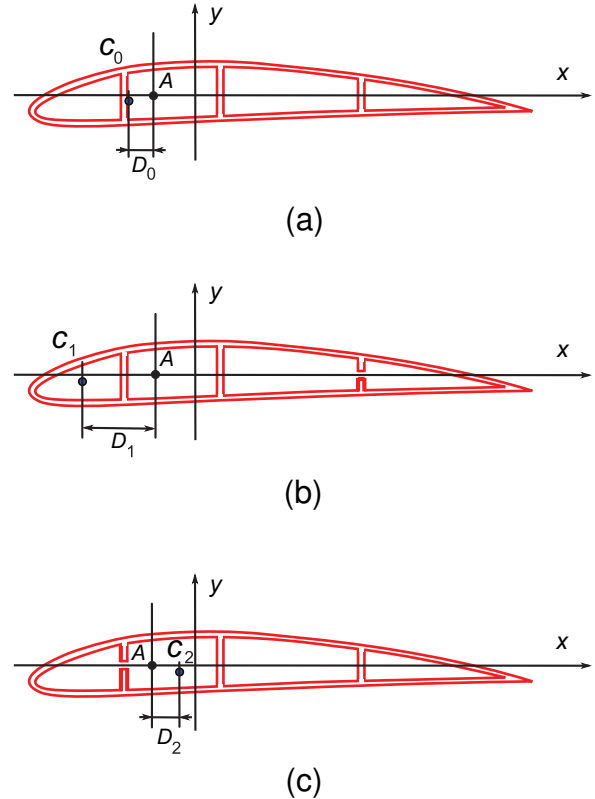


Figure 2. Cross sections with cut internal walls: (a) continuous walls, (b) front wall continuous and rear wall discontinuous, and (c) front wall discontinuous and rear wall continuous.

due to the torsional moment $M_{T,1} = D_1 Q_y$, is greater than the twist θ_0 . Likewise, if the front wall is uniformly cut as shown in Figure 2(c), the shear center is at the location C_2 and the twist θ_2 due to the torsional moment $M_{T,2} = D_2 Q_y$ is less than the twist θ_0 .

A small shift of the shear center is able to induce a large modification ΔD of the lever arm D and, in turn, a large modification of the torsional moment. If there were a technical device able to ensure or to break off the continuity of internal walls, it would be possible to modify and maybe control the twist of a profile.

In general, the transverse shear stresses τ_r and τ_f in the middle plane of the rear and front wall are not null, and they only vanish when the wall is discontinuous. In this case, the upper and lower parts of the cut wall exhibit a differential displacement Δw normal to the cross section (Figure 3(b)). The displacements for the rear and front walls are denoted by Δw_r and Δw_f . Depending on the state of the rear and front wall (continuous or discontinuous), there are four elementary configurations for the profile. Table 1 summarizes the values of the shear stresses and displacements for each configuration.

When a wall is discontinuous, tangential forces, whose resultant is null, can be applied to the edges of the cut wall (Figure 3(c)) to modify the displacement Δw . For example, in the configuration where the front wall of the profile is continuous and the rear wall is discontinuous (Figure 2(b)), if the tangential forces are

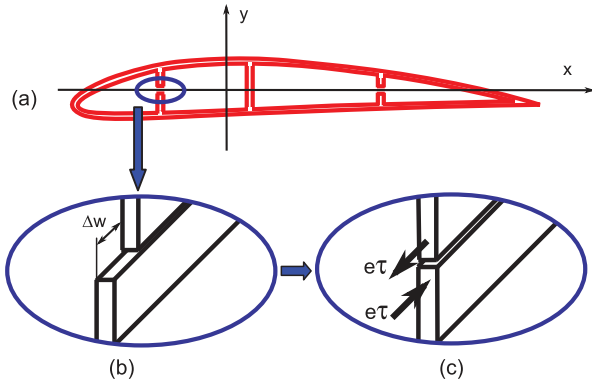


Figure 3. “Opening” and “closing” walls. (a) profile with discontinuous rear and front walls, (b) displacement Δw of a discontinuous wall and (c) closing of the wall by applying force in the same direction as the displacement Δw .

sufficient to impose a shear stress $\tau_r = \tau_{r,0}$ in the middle plane of the cut wall, the displacement would become $\Delta w_r = 0$. It is exactly as if the rear wall of the profile was continuous. Therefore, it is possible to change the configuration of the walls between “continuous” and “discontinuous” states. This change of state generates a modification of the torsional moment because it depends on the shear stresses τ_r and τ_f in the middle plane of the wall. It can be shown that the torsional moment also depends on the displacements Δw_r and Δw_f . The relations between the torsional moment M_T , shear stresses τ , and displacements Δw are linear and can be written as

$$\begin{cases} M_T = M_{T,3} + A_f \tau_f + A_r \tau_r \\ M_T = M_{T,0} + B_f \Delta w_f + B_r \Delta w_r \end{cases} \quad (4)$$

where A_f , A_r , B_f , and B_r are constants depending on the geometry of the cross section, and $M_{T,3}$ is the torsional moment when the front and rear walls are discontinuous.

The torsional moment M_T is in turn linked to the twist $\theta(z)$ by the relation

$$\frac{d\theta}{dz} = \frac{M_T}{GJ_{T,eff}} \quad (5)$$

where $GJ_{T,eff}$ is the effective torsional stiffness, which, in theory, depends on the configuration of the profile. Since the walls can be in a continuous or discontinuous state, the thin-walled cross section can be open or closed such that the torsional stiffness is included in the interval $[GJ_{T,3}, GJ_{T,0}]$. We assume that we know the relation between the effective torsional stiffness and the displacements Δw_r and Δw_f of the cut walls.

According to equations (4) and (5), it is theoretically possible to control the torsional moment and, in turn, the twist angle by controlling the displacements Δw of the internal walls using forces as shown in Figure 3(c). However, since the forces and the displacements are in the same direction, the work done by these external forces is not null and is always positive. This method, comparable to an active one, is therefore energy costly.

Proposed solution: a clutch-like system

To modify the state of the walls, we propose to use discontinuous walls whose upper and lower parts are

Table 1. Shear stresses (τ_f and τ_r) and displacements (Δw_f and Δw_r) for the four elementary configurations of the two walls.

		Rear wall			
		Continuous		Discontinuous	
Front wall	Continuous	$\tau_f = \tau_{f,0}$	$\tau_r = \tau_{r,0}$	$\tau_f = \tau_{f,1}$	$\tau_r = 0$
	Discontinuous	$\tau_f = 0$	$\tau_r = \tau_{r,2}$	$\tau_f = 0$	$\tau_r = 0$
		$\Delta w_f = 0$	$\Delta w_r = 0$	$\Delta w_f = 0$	$\Delta w_r = \Delta w_{r,1}$
		$\Delta w_f = \Delta w_{f,2}$	$\Delta w_r = 0$	$\Delta w_f = \Delta w_{f,3}$	$\Delta w_r = \Delta w_{r,3}$

compressed between two jaws (Figure 4). Rather than applying forces in the direction of the wall displacement Δw , pressure forces P are acting normally to this direction. The device attached to the wall is therefore comparable to a clutch system. The adaptive wall resulting from the assembly of the wall and the clutch-like system makes it possible to control the displacement Δw of the two parts of the wall by modifying the pressure forces P that lock or unlock the wall displacement.

More precisely, the control of the wall displacement is done as follows (Figure 5). First, the pressure force P_1 is sufficient to prevent the two parts of the adaptive wall to slide (Figure 5(a)), and the system is in an equilibrium state. The friction forces within the clutch are greater than the transverse shear forces applied to the wall. Then, if pressure forces are decreased from P_1 to P_2 , the friction forces decrease and the two parts of the wall may slide (Figure 5(b)) between the displacements 0 and Δw_{max} . Once the displacement set point Δw is achieved, the pressure forces are increased again from P_2 to P_1 (Figure 5(c)), such that the two parts of the wall do not slide anymore. A new equilibrium state is then obtained with the fixed displacement Δw .

In Figure 5(b), when the pressure forces are decreased, the variation of the displacement Δw occurs only if there is a shear force. This method is therefore effective only if external forces are applied to the

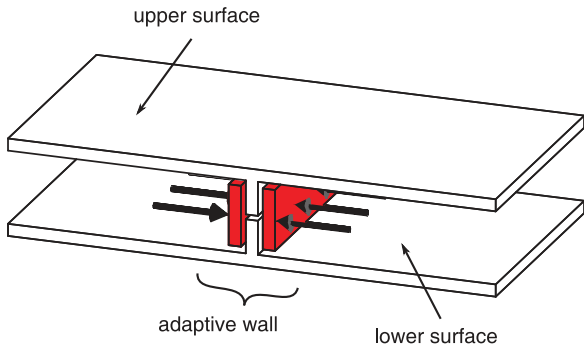


Figure 4. A clutch-like system.

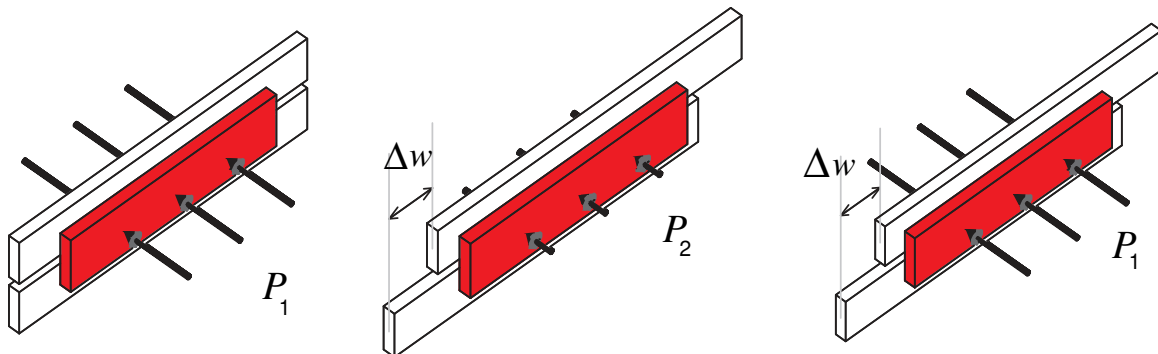


Figure 5. Mechanism of the clutch-like system: (a) no slide, (b) the normal forces decrease inducing a slide Δw , and (c) the displacement Δw is locked.

profile. That is why it is called a reactive control method. Compared to an active control, the reactive control described earlier has no need for a significant amount of external energy to change the configuration of the wall because the direction of the displacement Δw and the forces applied to the jaws are perpendicular.

Using these adaptive walls in an aerodynamic profile, it would be possible to control the displacements Δw_r and Δw_f of the rear and front walls from 0 to a maximum value. According to equations (4) and (5), this reactive control method would allow a twist control of the profile. By modifying the state of the rear wall, the twist angle would be increased and, inversely, it would be reduced by activating the front wall. It becomes apparent that if no twist control is required, the internal walls behave as if they were continuous. It means that the normal torsional behavior is the stiffest one.

Distribution of the clutch-like systems into the beam

Previously, the modifications of the continuity of the walls were uniform spanwise. By distributing clutch-like systems of length ΔL along the span direction (Figure 6) between the cross sections $\Sigma(z)$ and $\Sigma(z + \Delta L)$, it would be possible to control the differential twist angles $\Delta\theta_k = \theta_{k+1} - \theta_k$ of each elementary part of the beam. The twist control can then be refined by increasing the number of systems and/or varying their length ΔL .

Reactive twist control

We have established that the clutch-like system makes it possible to modify the twist, and that measurable internal displacements Δw define the state of the system. We call it the actuation system. To obtain a twist control system, we need to know the variations $\Delta\theta$ of the twist induced by the actuation. This relation can be experimentally determined by identifying the parameters B_r , B_f , and $GJ_{T,eff}$ of relations (4) and (5). It

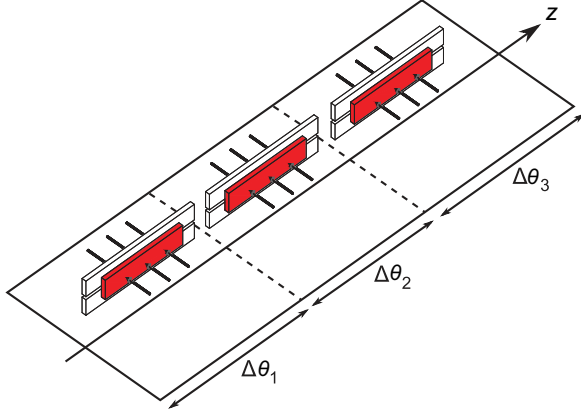


Figure 6. Example of distribution of the clutch-like systems along the span.

should be noted that it is not necessary to modelize the internal friction within the clutch.

Most of the time, the clutch system ensures the continuity of the walls and therefore is a locking system. In this configuration, the profile has the maximum torsional stiffness, and maintaining this stiffest state is not energy consuming. When a twist modification is needed, the clutch system is activated for a short period of time requiring only a very low amount of external energy. The activation of the system stops when the wall displacement has reached the set point corresponding to the desired twist angle.

In conclusion, the reactive twist control has a non-linear behavior, and the clutch-like system has two functions. First, it allows a possible twist control of the profile by measuring the internal displacements Δw , process designed to have the advantage of requiring a very low amount of external energy. Second, when the twist angle shifts to the desired one, the system is capable of locking it on to keep it at a constant value.

An example of the use of this system in an aerodynamic profile could be the following one:

Step 0: no aerodynamic forces are applied to the profile and the internal walls are locked. The twist angle of the structure is $\theta_0 = 0$.

Step 1: aerodynamic forces, relative to cruise flight conditions, for example, are applied to the profile. The walls are still locked and the twist angle is $\theta_1 \neq 0$.

Step 2: the clutch system is activated to modify the twist angle. When the optimum angle of attack is obtained, the twist angle is $\theta_2 \neq \theta_1$ and the clutch system is deactivated locking the twist of the profile.

Step 3: if a change occurs in the flight conditions, another activation of the system can be performed to adjust the twist angle: this will optimize again the angle of attack. The possibility of this second twist control depends on the chosen control strategy.

Indeed, depending on the order of activation of the internal systems, the walls can slide back.

Step 4: if aerodynamic forces become periodic with a very low-frequency-inducing vibrations of the profile, it would be possible to activate the clutch systems in a specific order to reduce the amplitude of those vibrations.

This reactive twist control method needs to be experimentally verified using demonstrators. In the following, experiments using three different demonstrators are presented showing the feasibility of this reactive control method. In these demonstrators, there will be one, two, or three adaptive walls in the cross section. The following notation has been chosen to simplify the description of the internal wall configuration

$$\text{configuration} = (\text{state}_1, \text{state}_2, \text{state}_3) \quad (6)$$

where state_n can be “close” or “open” meaning that the n th wall is continuous or discontinuous. The state_n is ranked in the order of increasing chord coordinate. For example, (open, close, close) is the configuration shown in Figure 2(c).

The clutch system of the first and second demonstrators is simplified because it is activated manually using screws to lock or unlock the walls. This simplification allows an easy manufacturing and is sufficient to verify the proof of concept. The third demonstrator uses a more elaborated clutch system that can be activated using an automated process.

A simplified mechanical system to control the twist angle

A first demonstrator has been designed to determine the variations of the twist angle $\Delta\theta$ that can be obtained using the reactive control as described previously. The purpose is to determine experimentally the order of magnitude of the variation $\Delta\theta$ with respect to the initial angle θ_0 .

Description of the demonstrator

The demonstrator is a cantilever beam of span 500 mm, chord 100 mm, and thickness 10 mm. Those dimensions are chosen such as their ratios correspond to the ones of typical aerodynamic profiles. As shown in Figure 7, the structure is composed of several identical parts along the span.

The internal structure is made of three walls whose adaptive mechanism is simplified compared to Figure 4 in order to ease the manufacturing of the demonstrator (Figure 8). On each cross section, there are three walls of remarkably large width made for screws to go through them and connect the upper and lower surfaces together (Figure 9). Therefore, the change of the

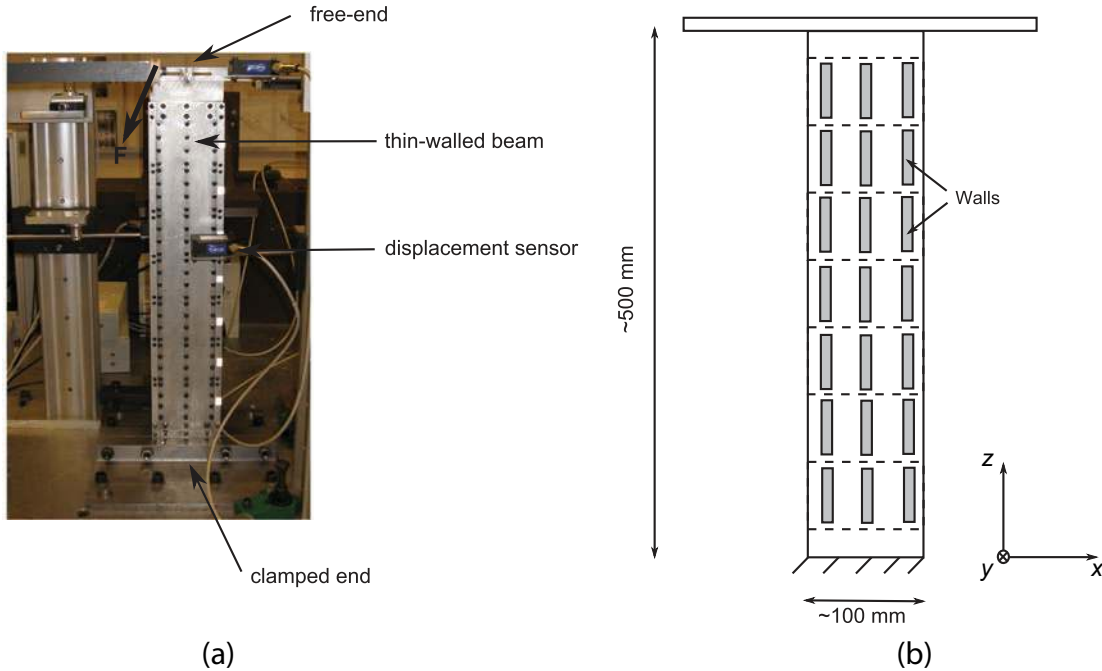


Figure 7. First demonstrator: (a) experimental setup and (b) structure of the demonstrator.

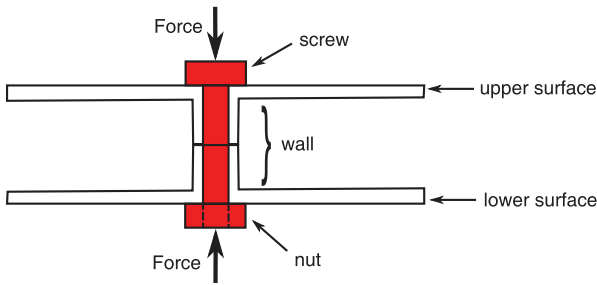


Figure 8. Simplified adaptive wall mechanism.

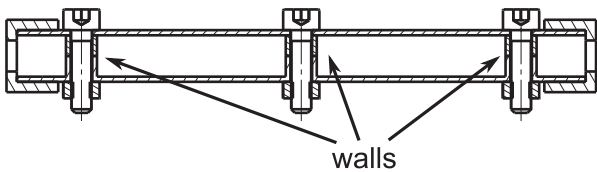


Figure 9. Typical cross section of the beam.

wall states is done manually by tightening or loosening the screws. This simple mechanism allows only the two states “open” and “close,” corresponding to $(\tau=0, \Delta w \neq 0)$ or $(\tau \neq 0, \Delta w=0)$ but it is sufficient to obtain a first proof of concept. Based on those results, the next demonstrators will be set up to take advantage of the intermediate displacements of the walls.

The purpose of this demonstrator is to determine the variation of the twist angle when a uniform modification of the continuity of one or several walls is

performed along the whole span. In this case, all the elementary parts of the structure have identical states.

Behavior of the structure

When the demonstrator is subjected to a transverse point force applied at its free-end, its deformation is bending and torsion. For a particular location of the applied force, displacements of selected cross sections are measured, such that their deflection and twist angle can be determined (Figure 7(a)). For each configuration of the internal structure, the results show that the deflection of the beam is correlated with a third-order polynomial curve and the rotation is linear with respect to the z -axis of the span and that is the expected theoretical behavior of a cantilever beam. An example of these curves in the configuration (open, open, open) is given in Figure 10. This configuration is assumed to be the least advantageous because of the residual internal friction coming from the opened walls. In conclusion, these experimental results show that despite the use of locking systems in the structure, the global behavior is the one of a cantilever beam.

It can be shown that the location of the shear center is at the middle of the cross section when the configuration is symmetrical (i.e. for the configurations (close, close, close), (close, open, close), (open, close, open), and (open, open, open)). For the asymmetrical configurations, the maximal displacement of the shear center happens when the closed walls are far away from the center of the cross section, that is, the configurations (open, open, close) and (close, open, open). For these

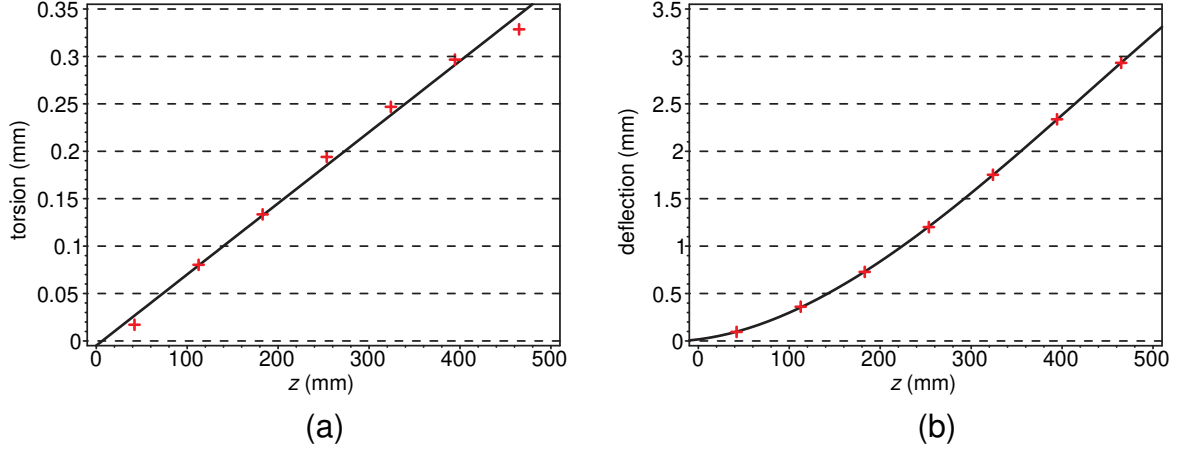


Figure 10. Behavior of the demonstrator in the configuration (open, open, open): (a) deflection of the beam and (b) rotation of the beam.

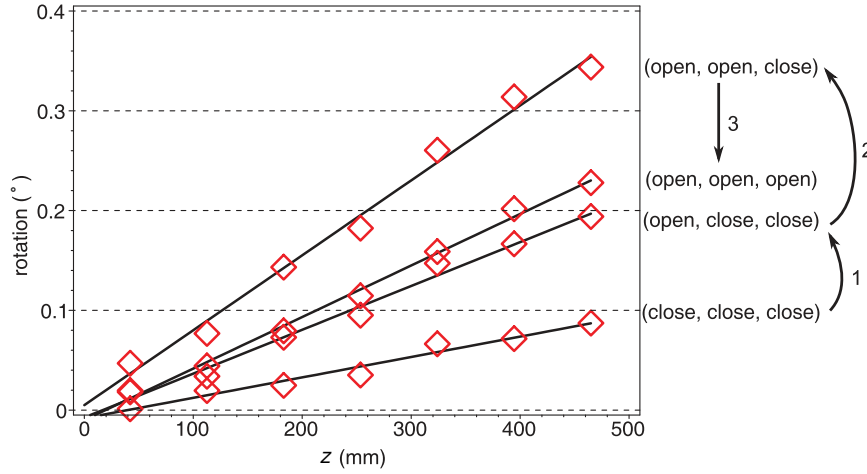


Figure 11. Rotations of the beam for each configuration of the sequence.

configurations, the shear center location has been experimentally determined: it is about ± 30 mm with respect to the middle of the cross section. Therefore, by opening walls, if the structure changes from a symmetrical configuration to an asymmetrical one, the shear center can be efficiently shifted to induce a large modification of the twist angle.

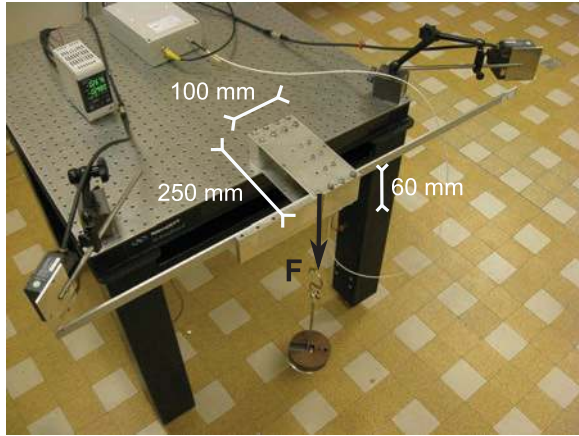
Experimental twist results

To determine the orders of magnitude of the variation of the twist angle, the following experiment has been performed. First, all the walls are closed and a point force is applied at the free-end, at 20% of the chord. The rotation of the whole beam is determined when the internal configuration is successively (close, close, close), (open, close, close), (open, open, close), and (open, open, open). The results are shown in Figure 11, and the twist angle at the free-end for each configuration is reported in Table 2. According to these

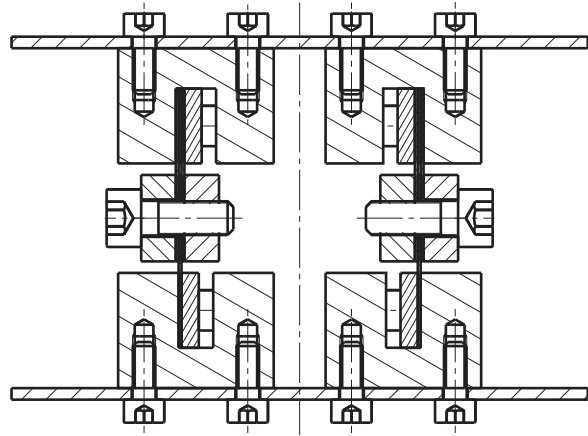
Table 2. Twist angles at the free-end for each configuration of the sequence.

Configuration	Twist angle θ (°)	Variation $\Delta\theta/\theta_0$
(close, close, close)	0.087	0
(open, close, close)	0.197	1.3
(open, open, close)	0.354	3.1
(open, open, open)	0.230	1.6

experimental results, from the configuration (close, close, close) to (open, open, close), the rotation increases significantly. This behavior is the one expected because, by opening the walls in this way, the shear center moves away from the middle of the beam inducing an increase of the torsional moment. This large change in the twist angle cannot only be explained by a modification of the torsional stiffness because the rotation of the configuration (open, open, open) is less than the one of the configuration (open, open, close).



(a)



(b)

Figure 12. Second demonstrator: study of the internal system: (a) experimental setup and (b) typical cross section of the demonstrator.

In conclusion, by changing the continuity of internal walls in a cantilever beam, it is possible to generate large variations of the twist angle. The order of magnitude of those variations is the same as the initial twist angle θ_0 .

Experimental study of the internal system

The simplified adaptive walls of the first demonstrator were not designed to allow a continuous twist control because only the states open and close of the walls were accessible. It is now proposed to study the internal system as described in Figure 5 and then to test its twist control feasibility by measuring the internal displacement Δw .

Description of the demonstrator

To study more precisely the mechanism of the internal system, a second demonstrator is designed: it looks like an elementary part of the first demonstrator but with a larger height, designed to integrate easily manual clutch-like systems. Despite the ratios of this demonstrator (Figure 12(a)), it is supposed to behave like a cantilever beam. There are two adaptive walls in the cross section, and their mechanism is the same as the one described in Figure 5. The four different configurations of the internal structure are as follows: (open, open), (open, close), (close, open), and (close, close).

Compared to the previous structure (Figure 7), this demonstrator allows the adaptive wall displacements to be measured. Since sensors are difficult to insert within the structure, the measurement is performed between the upper and lower skins (Figure 13).

Behavior of the structure

To study the behavior of the structure for each configuration, experiments are performed using a point force

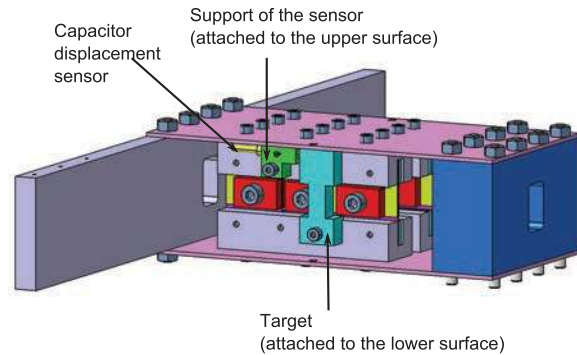


Figure 13. Measurement of the displacement of the wall.

applied at the free-end of the beam (Figure 12(a)) increasing from 0 to F , then decreasing from F to 0. For each configuration, the experimental results show that the rotation and the internal displacements depend linearly on the force, and that the unloading path does not show any hysteresis of the system (Figure 14).

The rotation versus force curve (Figure 14(a)) depends on the configuration of the internal structure. Its slope depends on the torsional stiffness and also on the shear center location. The difference between the slopes of the two curves may come from a large shift of the shear center.

When the adaptive wall is locked, the measured internal displacement is close to zero (Figure 14(b)). On the other hand, when the screws are loosening to open the wall, the displacement is much larger and can be measured.

Torsional characteristics

To determine experimentally the shear center location and the torsional stiffness of a cantilever beam, the

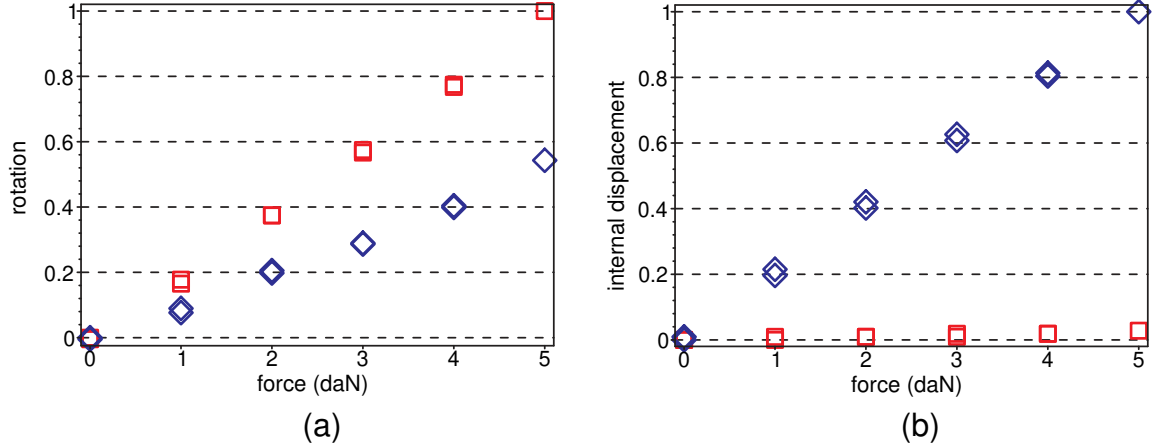


Figure 14. Example of the behavior of the structure in the configurations (close,close) (◇) and (open,close) (□): (a) rotation versus force curve and (b) internal displacement versus force curve.

method consists in measuring its twist when a point force is applied at two different points of the free-end. This method has been applied to the demonstrator, and the experimental results for its four configurations are shown in Figure 15.

The intersection between the straight lines and the x -axis is relative to the locations of the shear center, and the slope of the straight lines is relative to the torsional stiffness. These data are reported in Tables 3 and 4.

The variation of the torsional stiffness with respect to the one of the configuration (close, close) is defined as $\varepsilon = |GJ_T - GJ_{T,0}|/GJ_{T,0}$. The experimental results show that this variation is low (<20%), whereas the cross section is “open” in three of the configurations. We expected the torsional stiffness to be very different between the configuration (close, close) and the other configurations but this behavior can be explained by the nonuniform torsion theory of Vlassov. This low variation of the torsional stiffness is in favor of the twist control because it means that whatever the configuration of the structure, its dynamic is quite the same as the one of the normal configuration (close, close).

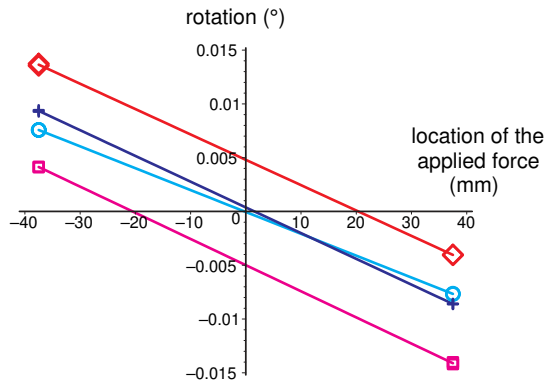


Figure 15. Determination of the torsional characteristics: (close, close) (○), (open, close) (◇), (close, open) (□), and (open, open) (+).

Concerning the shear center, its maximum displacement is about 20% of the beam width. These locations are the expected ones.

To show that this shift of the shear center is sufficient to modify significantly the twist angle, the following experiment is performed. A point force is applied step-by-step at the location +12.5 mm of the free-end. The rotation of the beam tip and the wall displacements are measured during this loading (Figure 16). For the first five steps, the configuration of the system is (close, close), and according to Table 3, the shear center is at location 0 mm. Between Steps 5 and 6, the applied force remains constant but the left wall is opened inducing a gap in the displacement curve of Figure 16(b) and a modification of the rotation. From this step, the configuration of the internal structure is (open, close), and according to the previous results (Table 3), the shear center is at location +20 mm, on the other side of the point force. Therefore, for the next modifications of the external force, the behavior of the structure is different. Whereas the rotation is increasing during the first steps, from the Step 6, it decreases and can even become negative.

Relation between the variations of rotation and the internal displacement

When the configuration of the structure is changing, there is not only a modification of the twist angle but also a variation of the internal displacements Δw , which can be measured. Using the clutch system of this demonstrator, it is difficult to determine the relation between these displacements and the rotation because the control of the wall slide is not possible using screws. However, the relation between these displacements and the rotation can be indirectly determined: a point force is applied at the free-end of the beam in the configuration (open, open). Four steps are performed as follows:

Table 3. Shear center locations.

Configuration	(close, close)	(open, close)	(close, open)	(open, open)
x_C (mm)	-0.23	+20.4	-20.5	+0.2

Table 4. Torsional stiffness GJ_T .

Configuration	(close, close)	(open, close)	(close, open)	(open, open)
GJ_T (Nm ²)	4370	3770	3650	3710
ε (%)	0	13.7	16.5	15.1

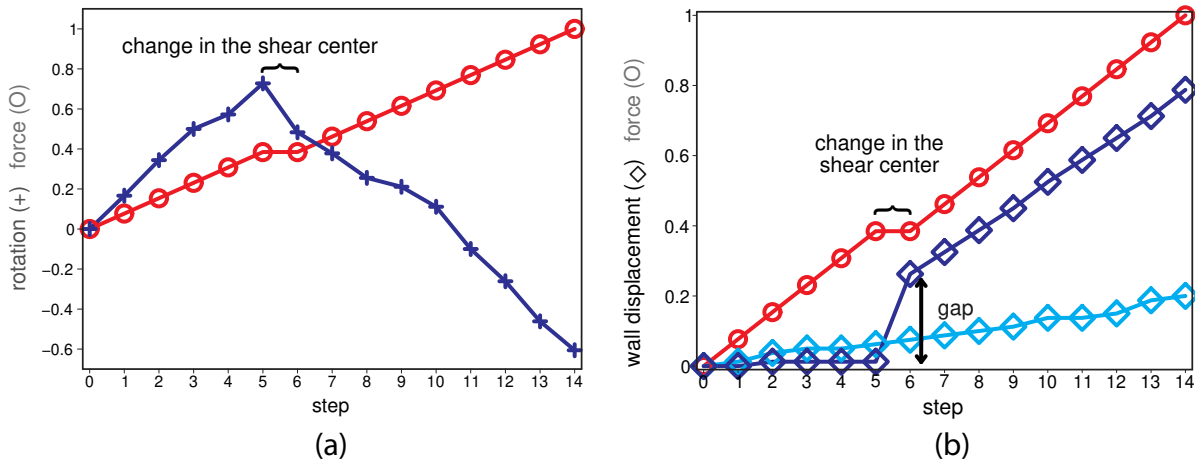


Figure 16. Experimental results illustrating the fact that a change in the internal configuration can generate significant modifications of the twist angle: (a) rotation at the free-end of the beam during the loading and (b) wall displacement during the same loading.

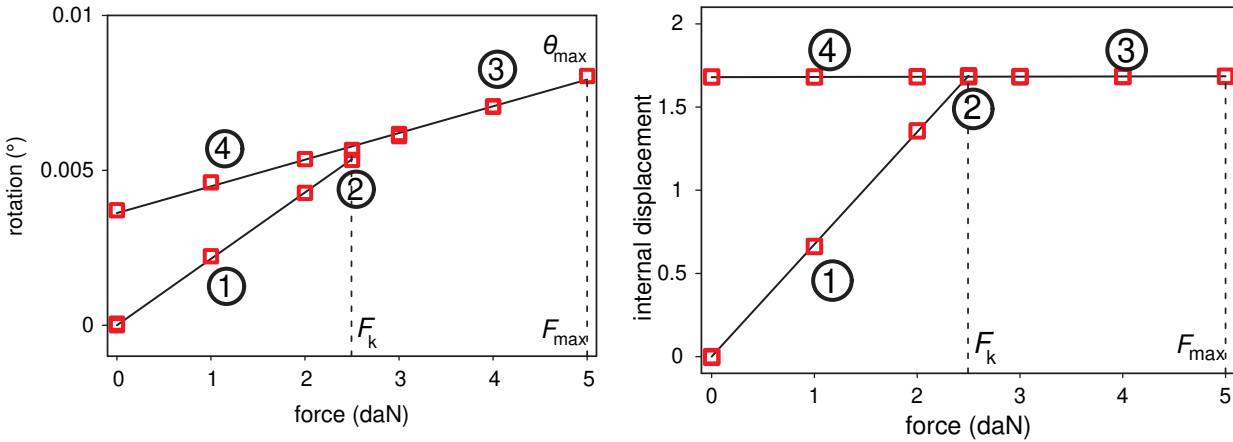


Figure 17. Example of experimental results showing the pattern of (a) the rotation versus external force curve and (b) the internal displacement versus external force curve.

1. Increase of the force from 0 to a transition force F_k
2. Locking of a clutch system (configuration (open, close)) with the applied force F_k
3. Increase of the force from F_k to $F_{max} = 5$ daN
4. Decrease of the force from F_{max} to 0.

As happened in the previous experiment, after the switch of the internal configuration, the slope of the rotation and the internal displacement curves change (Figure 17). Moreover, as expected, the locking of the clutch system (Step 2) does not induce any variation of the rotation; it only locks the wall displacement.

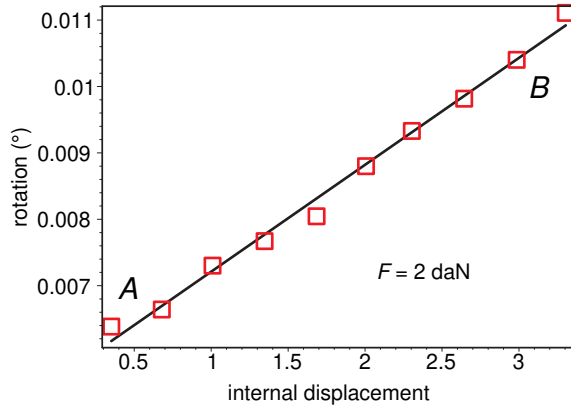


Figure 18. Relation between the rotation and the internal displacement.

This experiment can be performed using several transition force F_k . The pattern of the experimental results is always the same as the one of Figure 17. For each of these experiments, the rotation θ_{max} for the maximum force F_{max} depends on the value of the transition force F_k and therefore on the locked displacement of the wall. The rotation θ_{max} is plotted in Figure 18 as a function of the internal displacement.

For a given external force ($F = 2 \text{ daN}$ in the example of Figure 18), the relation between the twist angle and the internal displacement is linear. By opening a wall, the rotation can be modified from A to B , depending on the value of the internal displacement.

For other values of the external force, there are another linear relations that can also be experimentally determined.

Remote activation

Previously, the twist control system was activated manually using screws to simplify the manufacturing of

the demonstrators. The objective was to verify the feasibility and the effectiveness of the “reactive” method concept. Another demonstrator using a more elaborated activation system is now designed. It is described as remote activation to distinguish it from the previous manual one. It means that the system is activated from the outside of the demonstrator using an automated process, the pressure force being imposed to the clutch-like system by pneumatic jacks.

Test of an adaptive wall

A clutch-like system is designed as described in Figure 5. Its activation is done by pneumatic jacks, which are included in the lower part of the adaptive wall (Figure 19(a)). To verify its mechanism, this adaptive wall is inserted between two skins (Figure 19(b)) in a structure whose in-plane dimensions are the same as the ones of the second demonstrator (Figure 12) but its thickness is smaller (20 mm). A point force is applied at the free-end of this cantilever beam, and the rotation θ of the tip is measured. The internal displacement Δw is also measured while the clutch system is activated. Considering the design of the adaptive wall, it is difficult to measure the displacement of the wall, that is, the sliding between the two parts. Therefore, as mentioned for the second demonstrator (Figure 13), the measured displacement is in reality the displacement between the upper and lower skin.

To evaluate the feasibility of the reactive control using this adaptive wall, the following experiment is performed: starting from the configuration where the internal displacement is null, the clutch system is activated step-by-step allowing, for a moment, the wall to slide. Figure 20 shows a typical experimental result. Its curves define functions, which have several plateaus, corresponding to twist equilibrium states of the

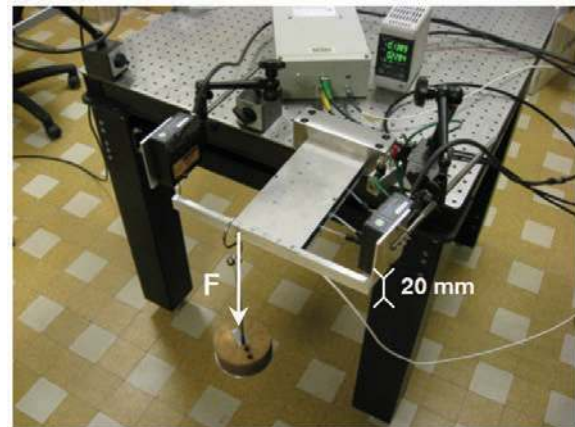
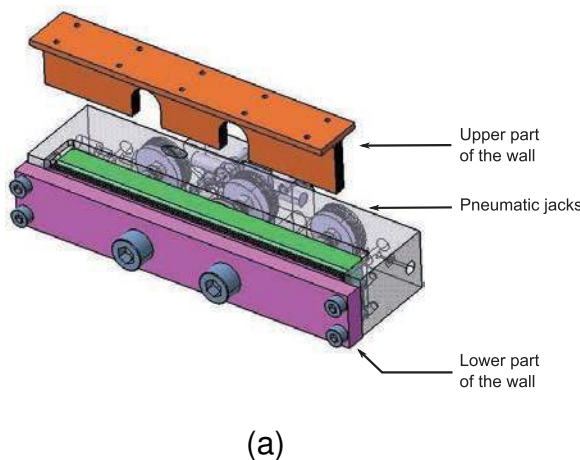


Figure 19. Demonstrator using an adaptive wall: (a) an adaptive wall allowing remote control and (b) experimental setup with only one adaptive wall in the structure.

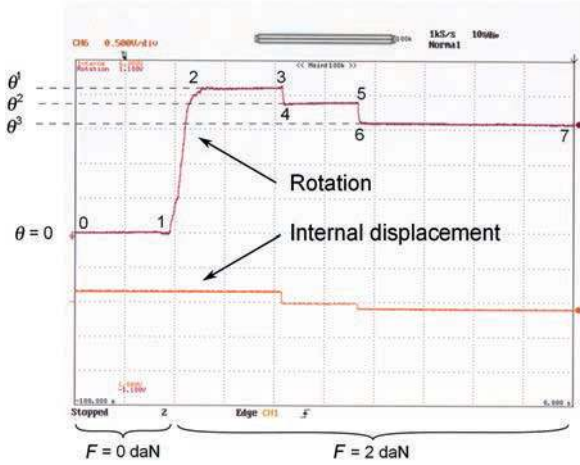


Figure 20. Example of an activation of the adaptive wall.

Table 5. Twist angles at the free-end during the experiment.

	External force (daN)	Twist angle ($^{\circ}$)
From 0 to 1	0	0
From 2 to 3	2	θ^1
From 4 to 5	2	$\theta^2 < \theta^1$
From 6 to 7	2	$\theta^3 < \theta^2 < \theta^1$

structure. In this experiment, the clutch system is activated two times (between Steps 3 and 4 and Steps 5 and 6), inducing variations of the internal displacement Δw . These results show that when the structure is subjected to a static force, it is possible to reduce the rotation of its free-end (Table 5). We can observe that no oscillations of the rotation occur between two plateaus, and the rotations are stable when the clutch system is locked.

In this experiment, the duration of the activation is very short and is not controlled. Therefore, if another experiment is performed, another values of the rotations θ^2 and θ^3 are obtained. According to the experimental results of Figure 18, if the internal displacement is controlled, it would be possible to reach all the rotations between θ^1 and θ^{min} , that is, the rotation obtained when the wall displacement is maximum.

In conclusion, using one adaptive wall in the structure, it is possible to modify the rotation in a monotonic way (a reduction of the rotation in the case of the experiment of Figure 20). To allow the rotation to increase or decrease, two adaptive walls must be inserted in the structure.

Demonstrator with two adaptive walls

A demonstrator using a complete remote activation system (two adaptive walls) is designed (Figure 21). It is a cantilever beam of span 1000 mm, chord 200 mm, and



Figure 21. Demonstrator using two adaptive walls.

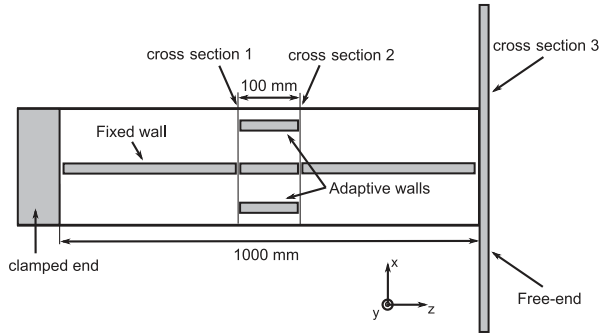


Figure 22. Scheme of the demonstrator.

thickness 20 mm. A wall is located in the middle of the width all along the span; it is always in the continuous state.

According to the scheme of Figure 22, the beam is divided into three parts. The first part, between the root and the cross section 1, contains only the central wall. The second (and central) part, between the cross sections 1 and 2, is about 100 mm long and contains a twin activation system, that is, two adaptive walls located symmetrically on both side of the central wall. As shown in Figure 3(a), there are front and rear adaptive walls. The third part, between the cross sections 2 and 3, contains only the central wall. The rotations of the cross sections 1, 2, and 3, with respect to the root of the beam, named θ_1 , θ_2 , and θ_3 , respectively, are measured using displacement sensors. Internal displacements Δw associated with each activation system are also measured.

Using this demonstrator, it is possible to control the local twist angle $\Delta\theta = \theta_2 - \theta_1$ of the beam by monitoring the internal displacements Δw .

Behavior of the structure

Some experiments are performed to study the behavior of the structure for each of the configurations (open,

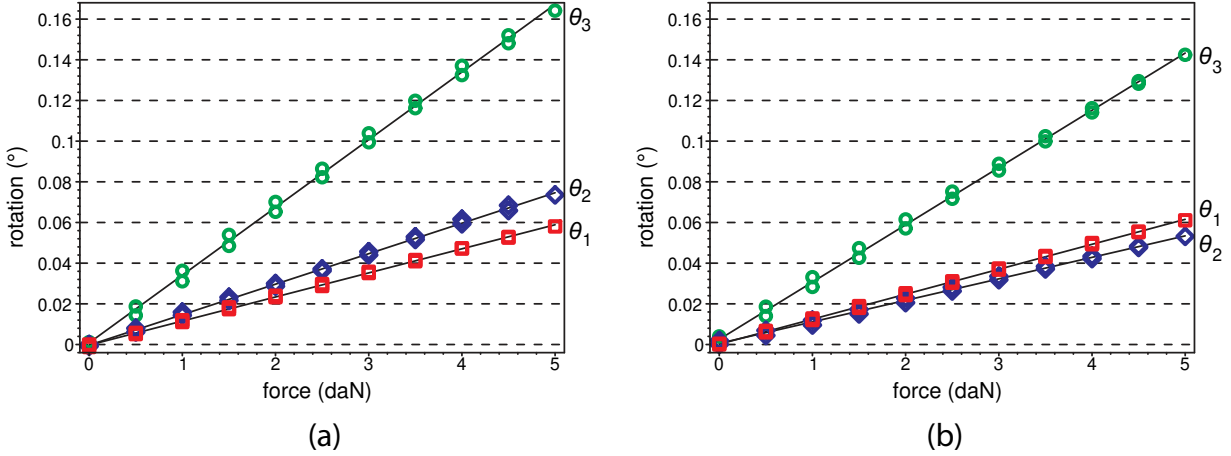


Figure 23. Rotations θ_1 (\square), θ_2 (\diamond), and θ_3 (\circ): (a) configuration (open, open) and (b) configuration (open, close).

open), (open, close), (close, open), and (close, close). The demonstrator is subjected to a point force applied at its free-end at about 30% chord. This force is increasing from 0 to a maximum force F and then decreasing from F to 0.

Figure 23(a) and (b) shows rotations versus force curves, respectively, for the configurations (open, open) and (open, close). The rotations depend linearly on the force, and the unloading path does not show any hysteresis. In Figure 23(a), the rotation of cross sections 1, 2, and 3 are in ascending order $\theta_1 < \theta_2 < \theta_3$, which makes sense. On the other hand, when a wall is in the close state, the order of these rotations is $\theta_2 < \theta_1 < \theta_3$ (Figure 23(b)). In this configuration, the shear center between cross sections 1 and 2 is shifted to the other side of the location of the applied point force, inducing an opposite torsional moment in this part of the beam.

According to Figure 23(a) and (b), the differential twist angles θ_1 and $\theta_3 - \theta_2$ of the first and third parts of the beam are independent from the configuration of the central part. Indeed, the variation of the rotation at

the free-end θ_3 corresponds to the variation of the differential rotation $\Delta\theta = \theta_2 - \theta_1$ obtained when the configuration is changed. It means that the activation of the system affects only the twist of the central part. To allow the twist to be controlled all along the span, it is necessary to use multiple adjacent parts in span direction as shown in Figure 6.

The internal displacement Δw of the adaptive wall that is activated between the configurations (open, open) and (open, close) is represented in Figure 24. The pattern of these experimental results is the same as the one obtained using the second demonstrator (Figure 14(b)). The curves show here a little hysteresis, which may be due to residual forces occurring during the mounting of the adaptive walls.

Determination of the shear center locations

The demonstrator has been designed to obtain large modifications of the shear center location in the central part of the beam when the adaptive walls are activated. According to the Vlassov theory, the maximum shear

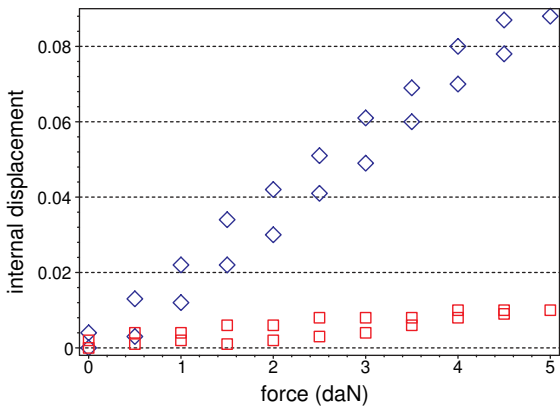


Figure 24. Variation of the internal displacement Δw : (open, open) (\diamond) and (open, close) (\square).

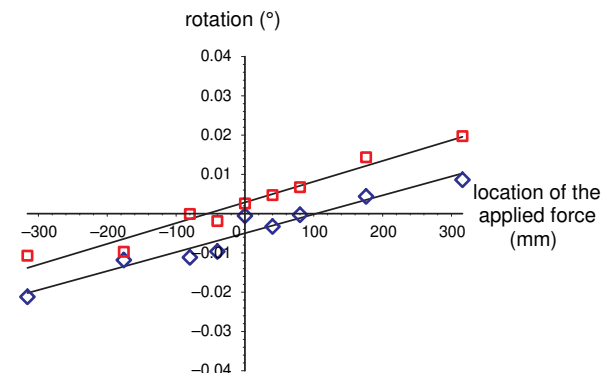


Figure 25. Determination of the torsional characteristics: (open, close) (\diamond) and (close, open) (\square).

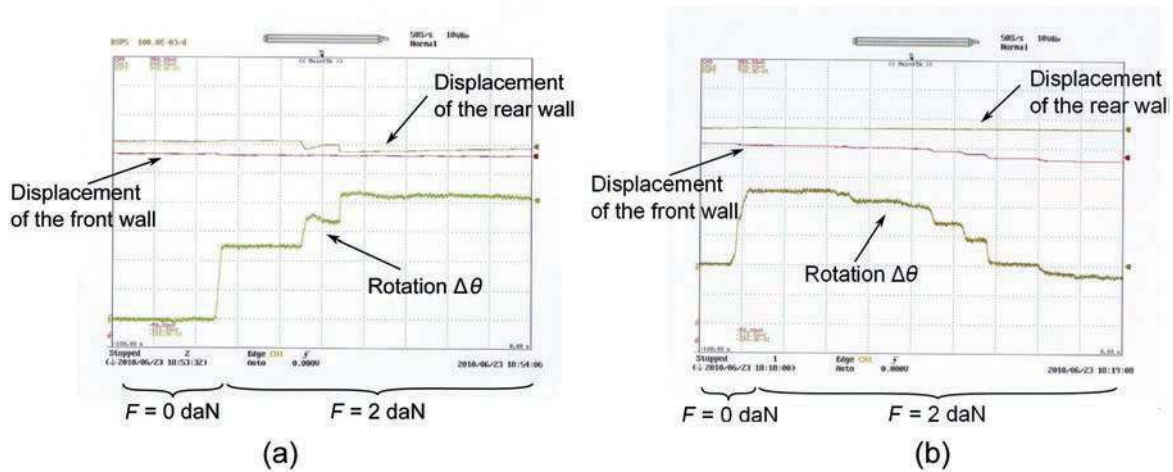


Figure 26. Feasibility of the static twist control: (a) increase of the rotation and (b) decrease of the rotation.

center location is theoretically located at ± 65 mm with respect to the middle of the cross section in the asymmetrical configurations (open, close) and (close, open). To determine experimentally these locations for each internal configuration, a point force is applied at different locations at the free-end of the beam, and the differential rotation $\Delta\theta = \theta_2 - \theta_1$ of the central part is estimated for each configuration. To make sure to evaluate correctly the twist angle $\Delta\theta$, a digital image correlation method is used to measure the twist angle. The results show that the out-of-plane displacements of the beam are typical of a flexion-torsion deformation, and that there is no local buckling of the skin.

For the configurations (open, close) and (close, open), the differential rotation $\Delta\theta$ is represented as a function of the location of the applied force. Figure 25 shows that the points are almost aligned. The least-squares straight line fits show that the maximal shear center locations are -54 and $+103$ mm.

First twist control results

This demonstrator allows the twist control to be studied using an open or quasi-open loop control. There are, for example, two different objectives that can be considered: when the structure is subjected to a static force, the objective can be to reduce the rotation to 0 so that the structure behaves as if it were rigid in torsion. On the other side, when the structure is subjected to a periodic force whose frequency is very low, the objective can be to keep the rotation constant.

Experiments are performed when the beam is subjected to a static force. The experimental results show that using two adaptive walls in the structure, it is possible to increase or decrease the differential rotation $\Delta\theta$ (Figure 26) and to maintain a static rotation (Figure 26).

Concerning the control of vibrations, the manufactured clutch-like system is not entirely satisfactory

because of undesired couplings, which can be suppressed in the future.

Conclusion

To control the twist of airfoils, we have proposed to insert adaptive walls in the structure. Using clutch-like systems, those walls can be continuous or discontinuous changing the topology of the cross sections. The shear center can be shifted by the activation of the clutch system inducing a modification of the twist angle, which can be controlled by measuring the displacement of the wall. This reactive method has the advantage of requiring a very low amount of external energy compared to an active method.

Demonstrators have been designed to verify the efficiency of the method. The experimental results show that it is possible to induce large modifications of the shear center location without changing significantly the torsional stiffness of the cantilever beam. Moreover, the rotation of the structure depends linearly on the internal wall displacements, which allows the twist to be controlled using this parameter.

A demonstrator has been manufactured including a part comprising two adaptive walls. When the beam is subjected to a static force, it has been verified that it is possible to increase or decrease the differential twist angle of this part and to maintain a constant static twist angle.

Acknowledgment and Funding

This study was supported by a PhD Grant from Délégation Générale de l'Armement (DGA, France).

References

Antcliff RR and McGowan A-MR (2000) Active control technology at NASA Langley Research Center. In:

- Proceedings of RTO AVT symposium on active control technology for enhanced performance operational capabilities of military aircraft, land vehicles and sea vehicles, RTO MP-051*, Braunschweig, Germany, 8–11 May 2000.
- Atulasimha J and Chopra I (2003) Behavior of torsional shape memory alloy actuators. In: *44th AIAA/ASME/ASCE/AHS structures, structural dynamics, and materials conference, AIAA 2003-1558*, Norfolk, VA, 7–10 April 2003.
- Barbarino S, Bilgen O, Ajaj RM, et al. (2011) A review of morphing aircraft. *Journal of Intelligent Material Systems and Structures* 22: 823–877.
- Bueter A, Ehlert U-C, Sachau D, et al. (2000) Adaptive rotor blade concepts: direct twist and camber variation. In: *Proceedings of RTO AVT symposium on active control technology for enhanced performance operational capabilities of military aircraft, land vehicles and sea vehicles, RTO MP-051*, Braunschweig, Germany, 8–11 May 2000.
- Chopra I (2002) Review of state of art of smart structures and integrated systems. *AIAA Journal* 40(11): 2145–2187.
- Cooper JE (2006) Adaptive stiffness structures for air vehicle drag reduction. In: *Multifunctional structures/integration of sensors and antennas, meeting proceedings RTO-MP-AVT-141*, Neuilly-sur-Seine, Vilnius, Lithuania, 2–4 October 2006, France, pp.15.1–15.12.
- Gandhi F (2009) *Centrifugal force actuated variable span helicopter rotor*. US Patent US2009290981.
- Mistry M, Gandhi F, Nagelsmit M, et al. (2011) Actuation Requirements of a warp-induced variable twist rotor blade. *Journal of Intelligent Material Systems and Structures* 22: 919–933.
- Pendleton E (2000) Back to the future how active aeroelastic wings are a return to aviation’s beginnings and a small step to future bird-like wings. In: *Proceedings of RTO AVT symposium on active control technology for enhanced performance operational capabilities of military aircraft, land vehicles and sea vehicles, RTO MP-051*, Braunschweig, Germany, 8–11 May 2000.
- Riemenschneider J, Keye S, Wierach P and Mercier Des Rochettes, H. (2004) Overview of the common DLR/ONERA project active twist blade (ATB). In: *Proceedings of the 30th European rotorcraft forum*, Marseille, France, 14–16 September 2004.
- Wierach P, Riemenschneider J and Keye S (2005) Development of an active twist rotor blade with distributed actuation and orthotropic material. In: *Proceedings of SPIE, San Diego, CA, 10 March 2005*, vol. 5764, pp.183–191, Smart Structures and Materials 2005: Smart Structures and Integrated Systems Alison B. Flatau.